A Computational Study on the Reaction Mechanism of the Boulton−Katritzky Rearrangement

Frank Eckert and Guntram Rauhut*

Contribution from the Institut für Theoretische Chemie, Universität Stuttgart, Pfaffenwaldring 55, 70569 Stuttgart, Germany

Received May 18, 1998

Abstract: A detailed *ab initio* and density functional study of the Boulton−Katritzky rearrangement is presented. Two different reaction paths for the rearrangement of 4-nitrobenzofuroxan were investigated at the RHF, MP2, MP4(SDQ), B3-LYP, and BH&H-LYP levels, with further energy refinements using coupled-cluster theory (CCSD and CCSD(T)). Electron correlation effects appear to be extremely important both for geometries and for relative energies. All methods indicate a one-step mechanism. In agreement with experimental results, a recently discussed tricyclic intermediate could not be found.

1. Introduction

The Boulton−Katritzky rearrangement (BKR) has been well-known since the early 60's[1,2] and is still used widely in heterocyclic chemistry (for reviews see refs 3−9). Many syntheses rely on the BKR as a tool for the generation of new compounds.[6,10−13] The substituted benzo derivatives of 1,2,5-oxadiazoles involved are of significant importance for pharmaceuticals and as analytical reagents. The molecular class of benzofuroxans has a key function in many biological processes. Antibacterial and fungicidal activities have been reported for these compounds. In particular, nitrobenzofuroxans inhibit nucleic acid and protein biosyntheses. Nitro derivatives of benzofuroxan, synthesized the first time as early as 1899,[14] have also been investigated as promising materials in energetics and combustion chemistry.[15]

The BKR has been examined mechanistically in some detail, and it was shown that it could be generalized[2,16,17] to a class of bicyclic rearrangements as shown in Figure 1. However, the exact reaction mechanism of the BKR is not yet understood fully.[6] Through flash experiments, the BKR was found to be a thermally induced reaction only, whereas photolyzation leads to the well-known ring-chain tautomerism of benzofuroxans.[18] The balance of the equilibrium of the BKR in substituted nitrobenzofuroxans depends on steric, electronic, conformational, and strain effects.[10,11] On experimental evidence, a mechanism has been discussed for 4-nitrobenzofuroxan (**1**) as shown in Figure 2. However, intermediate **2** depicted in this scheme could not be trapped so far and has thus been turned down.[6] Quantum chemical calculations should provide insight into the actual mechanism.

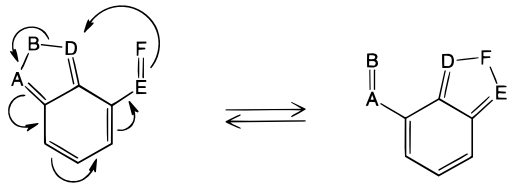

Figure 1. A generalized scheme of the Boulton−Katritzky rearrangement: A, E = N, N^+-O^-, N^+-N^-R, CR; B, F = O, NR, S; D = N, CR.

The unsubstituted benzofuroxan and its ring-chain tautomerism *via o*-dinitrosobenzene has been studied semiempirically[19] by *ab initio* Hartree−Fock (RHF), and by second-order Møller−Plesset (MP2) calculations, using basis sets ranging from 3-21G to pVTZ.[19−21] Density functional theory (DFT) has also been used to describe the tautomerism[21] and the vibrational spectra of the species involved.[22] DFT calculations using the B3-LYP exchange-correlation functional with the 6-311G(d,p) basis set were in best agreement with experimental geometries and activation energies for the reaction,[21] whereas the RHF and MP2 theory failed to represent the structure of benzofuroxan reliably and semiempirical methods performed even worse. Substituted

* To whom correspondence should be addressed: rauhut@theochem.uni-stuttgart.de.

(1) Boulton, A. J.; Katritzky, A. R. *Proc. Chem. Soc.* **1962**, 257.
(2) Boulton, A. J.; Ghosh, P. B.; Katritzky, A. R. *Angew. Chem. Int. Ed. Engl.* **1964**, *3*, 693.
(3) Boulton, A. J.; Ghosh, P. B. *Adv. Heterocycl. Chem.* **1969**, *10*, 1.
(4) Gasco, A.; Boulton, A. J. *Adv. Heterocycl. Chem.* **1981**, *29*, 251.
(5) Śliwa, W.; Thomas, A. *Heterocycles* **1985**, *23*, 399.
(6) Katritzky, A. R.; Gordeev, M. F. *Heterocycles* **1993**, *35*, 483.
(7) Katritzky, A. R. *J. Heterocycl. Chem.* **1994**, *31*, 569.
(8) Friedrichsen, W. Reactivity of Heterocyclic Ring. In *Houben-Weyl, Methoden der Organischen Chemie;* Schaumann, E., Ed.; Thieme: Stuttgart, 1994; Vol. E8c.
(9) Paton, R. M. 1,2,5-Oxadiazoles. In *Comprehensive Heterocyclic Chemistry II;* Katritzky, A. R., Rees, C. W., Scriven, E. F. V., Eds.; Pergamon Press: New York, 1995; Vol. 4.
(10) Takakis, I. M.; Hadjimihalakis, P. M. *J. Heterocycl. Chem.* **1992**, *29*, 121.
(11) Takakis, I. M.; Hadjimihalakis, P. M.; Tsantali, G. G.; Pilini, H. *J. Heterocycl. Chem.* **1992**, *29*, 123.
(12) Takakis, I. M.; Hadjimihalakis, P. M. *J. Heterocycl. Chem.* **1991**, *28*, 1373.
(13) Takakis, I. M.; Hadjimihalakis, P. M.; Tsantali, G. G. *Tetrahedron* **1991**, *47*, 7157.
(14) Droste, P. *Ann. Chem.* **1899**, *313*, 299.
(15) Oyumi, Y.; Brill, T. B. *Combust. Flame* **1986**, *65*, 313.
(16) Boulton, A. J.; Ghosh, P. B.; Katritzky, A. R. *J. Chem. Soc. (B)* **1966**, 1004.
(17) Boulton, A. J.; Ghosh, P. B.; Katritzky, A. R. *J. Chem. Soc. (B)* **1966**, 1011.
(18) Calzaferri, G.; Gleiter, R.; Knauer, K.-H.; Martin, H.-D.; Schmidt, E. *Angew. Chem. Int. Ed. Engl.* **1974**, *13*, 52.
(19) Friedrichsen, W. *J. Phys. Chem.* **1994**, *98*, 12933.
(20) Ponder, M.; Fowler, J. E.; Schaefer, H. F. *J. Org. Chem* **1994**, *59*, 6431.
(21) Rauhut, G. *J. Comput. Chem.* **1996**, *17*, 1848.
(22) Rauhut, G.; Jarzecki, A.; Pulay, P. *J. Comput. Chem.* **1997**, *18*, 489.

10.1021/ja981720x CCC: $15.00
Published on Web 12/30/1998

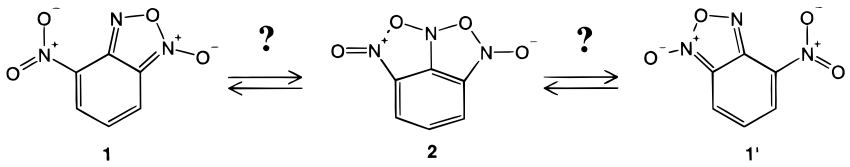

Figure 2. A possible reaction mechanism of the rearrangement of 4-nitrobenzofuroxan.

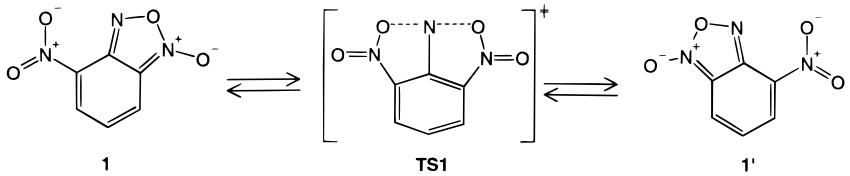

Figure 3. Reaction path A as investigated in this study.

benzofuroxans and the BKR have not yet been investigated by quantum chemistry methods.

Considering 4-nitrobenzofuroxan (**1**) as a prototype component of the BKR, two possible reaction pathways of the BKR were investigated in this study. Figure 3 shows a reaction path A proceeding in a single step via a symmetric transition state **TS1**. Figure 4 depicts a reaction path B with three stable intermediates, two of them being identical due to symmetry relations. In the first step, **1** opens its furazan ring via a nonplanar transition state to yield 1,2-dinitroso-3-nitro-benzene (**3**). This step corresponds to the ring-opening in the ring-chain tautomerism of benzofuroxans. In the following step, an oxygen atom is interchanged between the nitro and the nearest nitroso group to generate, again via an asymmetric transition state, the intermediate 1,3-dinitroso-2-nitro-benzene (**4**), which shows C_2 or C_{2v} symmetry, respectively (i.e., the oxygens of the nitro group lie perpendicular to the ring plane). The following two steps are identical to the first two.

On the basis of experience from previous studies of the benzofuroxan tautomerism,[19−21] this study is based mainly on density functional techniques and *ab initio* calculations including electron correlation. As these studies indicate, very high levels of theory are necessary for describing these electron-overcrowded molecules, which are known to be extremely correlation sensitive.[23,24]

2. Computational Details

All structures were optimized at five levels of theory, namely RHF, frozen-core MP2, frozen-core MP4 without triple excitations (i.e. MP4(SDQ)), and two DFT techniques (B3-LYP and BH&H-LYP). B3-LYP denotes Becke's three-parameter exchange functional[25] in combination with the correlation functional of Lee, Yang, and Parr.[26,27] BH&H-LYP denotes Becke's hybrid "half and half" method.[28] It has been shown by several groups that, within the density functional framework, the B3-LYP functional yields the best results for geometries and harmonic frequencies of polyatomic molecules[29−35] while underestimating reaction barriers.[36,37] On the contrary, the BH&H-LYP functional has been shown to reproduce reaction barriers especially well.[37−39] For both functionals, it is true that they capture a significant amount of dynamical as well as nondynamical correlation energy and are comparable to or even better than low-level *ab initio* correlation methods like MP2 or CISD.[34,40,41] This is of particular importance for the reactions considered here. Note that, for modern (gradient corrected) density functional theory as used here, nondynamical correlation is seized by the exchange functional, while the dynamical contribution is accounted for by the correlation functional.[42,43] All calculations presented here were carried out with the MOLPRO *ab initio* program package[44] except the DFT calculations and MP4 geometry optimizations which were done with the Gaussian suite of programs.[45]

Geometries of all stable structures and all transition states were optimized[46] at these levels of theory, and additionally, zero-point vibrational energies were calculated for all methods. In each case, the 6-31G* basis set[47] was used. For technical reasons, MP4(SDQ)/6-31G* frequency calculations could not be performed. To test for basis set effects, additional geometry optimizations for reference structure **1** were carried out with two different valence triple-ζ plus polarization basis

(23) Calleri, M.; Ranghino, G.; Ugliengo, P.; Viterbo, D. *Acta Crystallogr.* **1986**, *B42*, 84.
(24) Seminario, J. M.; Concha, M. C.; Politzer, P. *J. Comput. Chem.* **1992**, *13*, 177.
(25) Becke, A. D. *J. Chem. Phys.* **1993**, *98*, 5648.
(26) Lee, C.; Yang, W.; Parr, R. G. *Phys. Rev. A* **1988**, *38*, 3098.
(27) Miehlich, B.; Savin, A.; Stoll, H.; Preuss, H. *Chem. Phys. Lett.* **1989**, *157*, 200.
(28) Becke, A. D. *J. Chem. Phys.* **1993**, *98*, 1372.
(29) Rauhut, G.; Pulay, P. *J. Phys. Chem.* **1995**, *99*, 3093.
(30) Rauhut, G.; Pulay, P. *J. Phys. Chem.* **1995**, *99*, 14572.
(31) Scott, A. P.; Radom, L. *J. Phys. Chem.* **1996**, *100*, 16502.
(32) El-Azhary, A. A. *J. Phys. Chem.* **1996**, *100*, 15056.
(33) Lee, S. Y.; Boo, B. H. *J. Phys. Chem.* **1996**, *100*, 15073.
(34) Zuilhof, H.; Dinnocenzo, J. P.; Reddy, A. C.; Shaik, S. *J. Phys. Chem.* **1996**, *100*, 15774.
(35) Csonka, G. I.; Nguyen, N. A.; Kolossováry, I. *J. Comput. Chem.* **1997**, *18*, 1534.
(36) Glukhovtsev, M. N.; Bach, R. D.; Pross, A.; Radom, L. *Chem. Phys. Lett.* **1996**, *260*, 558.
(37) Bell, R. L.; Tavaeras, D. L.; Truong, T. N.; Simons, J. *Int. J. Quantum Chem.* **1997,** *63*, 861.
(38) Truong, T. N.; Duncan, W. T.; Bell, R. L. In *Chemical Applications of Density Functional Theory;* Laird, B. B., Ross, R. B., Ziegler, T., Eds.; American Chemical Society: Washington, 1996.
(39) Zhang, Q.; Bell, R. L.; Truong, T. N. *J. Phys. Chem.* **1995**, *99*, 592.
(40) Labanowski, J. K.; Andzelm, J. W. *Density Functional Methods in Chemistry;* Springer: New York, 1991.
(41) Ernzerhof, M.; Perdew, J.; Burke, K. Density Functionals: Where Do They Come From? Why Do They Work? In *Topics in Current Chemistry;* Nalewajski, R. F., Ed.; Springer: New York, 1996; Vol. 180.
(42) Gritsenko, O.; Schipper, P.; Baerends, E. *J. Chem. Phys.* **1997**, *107*, 5007.
(43) Baerends, E.; Gritsenko, O. *J. Phys. Chem.* **1997**, *101*, 5383.
(44) MOLPRO is a package of *ab initio* programs written by H.-J. Werner and P. J. Knowles, with contributions from R. D. Amos, A. Berning, D. L. Cooper, M. J. O. Deegan, A. J. Dobbyn, F. Eckert, C. Hampel, T. Leininger, R. Lindh, A. W. Lloyd, W. Meyer, M. E. Mura, A. Nicklass, P. Palmieri, K. Peterson, R. Pitzer, P. Pulay, G. Rauhut, M. Schütz, H. Stoll, A. J. Stone, and T. Thorsteinsson. Version 97.4, University of Birmingham, UK, 1997 (see http://www.tc.bham.ac.uk/molpro/).
(45) Gaussian 94, Revision D.1, M. J. Frisch, G. W. Trucks, H. B. Schlegel, P. M. W. Gill, B. G. Johnson, M. A. Robb, J. R. Cheeseman, T. Keith, G. A. Petersson, J. A. Montgomery, K. Raghavachari, M. A. Al-Laham, V. G. Zakrzewski, J. V. Ortiz, J. B. Foresman, J. Cioslowski, B. B. Stefanov, A. Nanayakkara, M. Challacombe, C. Y. Peng, P. Y. Ayala, W. Chen, M. W. Wong, J. L. Andres, E. S. Replogle, R. Gomperts, R. L. Martin, D. J. Fox, J. S. Binkley, D. J. Defrees, J. Baker, J. P. Stewart, M. Head-Gordon, C. Gonzalez, and J. A. Pople, Gaussian, Inc.: Pittsburgh PA, 1995".
(46) Eckert, F.; Pulay, P.; Werner, H. J. *J. Comput. Chem.* **1997**, *18*, 1473.
(47) Ditchfield, R.; Hehre, W. J.; Pople, J. A. *J. Chem. Phys.* **1971**, *54*, 724.

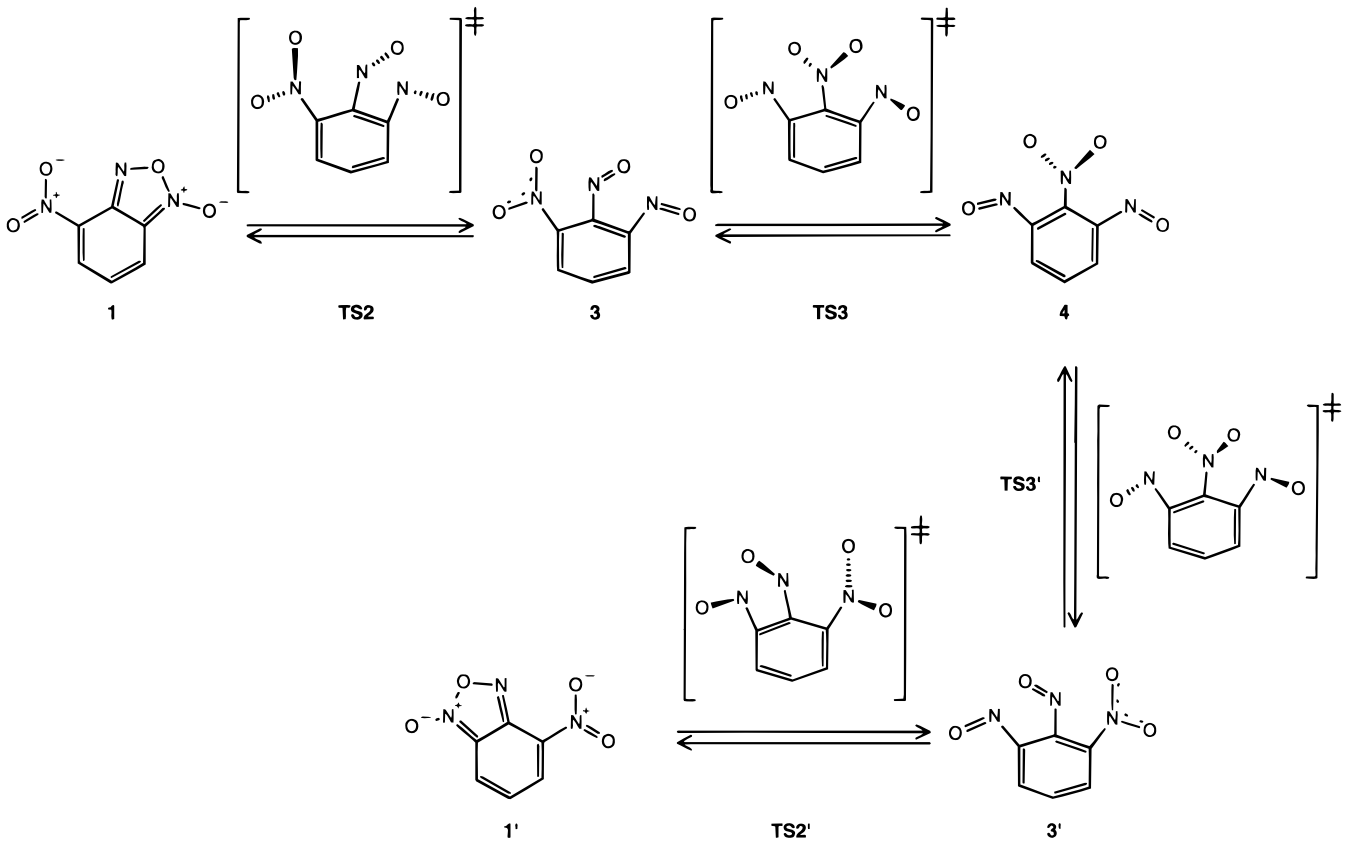

Figure 4. Reaction path B as investigated in this study.

sets, namely the 6-311+G* and the 6-311G(2df,p) bases.[48] The first basis was used in combination with RHF, MP2, B3-LYP, and BH&H-LYP theory, while the latter was used in combination with the B3-LYP functional only. Transition states were verified by tracing down the intrinsic reaction path (IRC) from the saddle points to the neighboring energy minima. This was done by using Sun and Ruedenberg's quadratic steepest descent method[49,50] as implemented in MOLPRO,[44] or in case of the DFT calculations, by using the algorithm of Gonzalez and Schlegel as implemented in Gaussian 94.[51]

To include higher electron correlation effects, single-point energy calculations were performed for both mechanisms. For reaction A, MP4-(SDTQ), CCSD, and CCSD(T) calculations (i.e., coupled-cluster calculations with single and double excitations and perturbational triples [CCSD(T)][52]) on top of B3-LYP and MP4(SDQ) optimized structures were carried out. CCSD and CCSD(T) single-point calculations were also performed for all structures of mechanism B, which show lower symmetry.

The quality of the 6-31G* basis is relatively low in comparison with the quality of the correlation methods applied. For this reason, the larger 6-311G(2df,p) basis was used in combination with MP2 and MP4-(SDQ) calculations to study basis set effects on the activation barrier of reaction A. We consider the CCSD(T)/6-31G* and MP4(SDQ)/6-311G(2df,p) calculations the most reliable ones for the reactions investigated.

3. Reaction Path A

Reaction path A is closely related to the mechanism discussed by Katritzky and Gordeev.[6] However, in agreement with these authors an intermediate structure **2** (see Figure 2) could not be found by systematic scans of the potential energy surface, but a transition state of formally the same geometry was identified.

3.1. Geometries. Geometric parameters of 4-nitrobenzofuroxan (**1**), the only stable structure involved in reaction mechanism A, are shown in Table 1. As can be expected, all functionals and methods used (i.e., B3-LYP, BH&H-LYP, RHF, MP2, and MP4) in combination with a 6-31G* basis provide C_s symmetry for this structure. The labeling of the atoms is given in Figure 5. Direct comparison of these geometric parameters with experimental data for this prototype reaction is not possible, since crystallographic data are available only for benzofuroxan,[53] substituted benzofuroxans other than nitrobenzofuroxans[54−57] or 4,6-dinitrobenzofuroxan,[58] and substituted 4,6-dinitrobenzofuroxans.[59,60] However, for all of these compounds, the most critical bond lengths, i.e., the endocyclic N−O bonds of the furazan ring (N_1-O_2 and N_2-O_2), are within the ranges of 1.38−1.42 Å for N_1-O_2 and 1.41−1.48 Å for N_2-O_2,[4] respectively. It has been shown by several authors[19−21] that *ab initio* calculations primarily have problems in describing the N_2-O_2 bond since dynamical correlation has an extreme impact on this parameter. Table 1 reflects this finding.

As can be seen from Table 1, MP4(SDQ) calculations and the B3-LYP functional probably provide the most reliable

(48) Krishnan, R.; Binkley, J. S.; Seeger, R.; Pople, J. A. *J. Chem. Phys.* **1980**, *72*, 650.
(49) Sun, J. Q.; Ruedenberg, K. *J. Chem. Phys.* **1993**, *99*, 5257.
(50) Sun, J. Q.; Ruedenberg, K. *J. Chem. Phys.* **1993**, *99*, 5269.
(51) Gonzalez, C.; Schlegel, H. B. *J. Phys. Chem.* **1990**, *94*, 5523.
(52) Hampel, C.; Peterson, K.; Werner, H. J. *Chem. Phys. Lett.* **1992**, *190*, 1.
(53) Britton, D.; Olson, J. *Acta Crystallogr., Sect. B* **1979**, *35*, 3076.
(54) Britton, D.; Hardgrove, G.; Hegstrom, R.; Nelson, G. *Acta Crystallogr., Sect. B* **1972**, *28*, 1121.
(55) Gehrz, R.; Britton, D. *Acta Crystallogr., Sect. B* **1972**, *28*, 1126.
(56) Britton, D. *Acta Crystallogr., Sect. C* **1992**, *48*, 1283.
(57) Britton, D.; Noland, W. *Acta Crystallogr., Sect. B* **1972**, *28*, 1116.
(58) Prout, C.; Hodder, O.; Viterbo, D. *Acta Crystallogr., Sect. B* **1972**, *28*, 1523.
(59) Ramm, M.; Schulz, B.; Rudert, R.; Gohrmann, B.; Niclas, H.-J. *Acta Crystallogr., Sect. C* **1991**, *47*, 1700.
(60) Ramm, M.; Niclas, H.-J.; Gohrmann, B. *Z. Kristallogr.* **1992**, *200*, 189.

Table 1. Geometric Parameters of 4-Nitrobenzofuroxan (C_s) **1**

r^a	RHF	MP2	MP4[b]	B3-LYP	BH&H[c]	angles	RHF	MP2	MP4[b]	B3-LYP	BH&H[c]
C_1-C_2	1.419	1.405	1.425	1.429	1.417	$C_1-C_2-C_3$	125.0	124.2	124.8	124.6	125.0
C_2-C_3	1.423	1.405	1.428	1.411	1.408	$C_2-C_3-C_4$	116.3	116.4	116.1	116.6	116.4
C_3-C_4	1.344	1.383	1.362	1.373	1.357	$C_3-C_4-C_5$	120.9	121.5	121.4	121.0	120.9
C_4-C_5	1.446	1.416	1.448	1.429	1.428	$C_4-C_5-C_6$	123.0	120.8	122.1	122.3	122.6
C_5-C_6	1.346	1.378	1.360	1.371	1.356	$C_5-C_6-C_1$	118.9	119.9	119.5	119.3	119.1
C_6-C_1	1.445	1.418	1.446	1.436	1.432	$C_6-C_1-C_2$	115.9	117.2	116.2	116.2	116.0
C_1-N_1	1.288	1.376	1.322	1.325	1.306	$C_2-N_2-O_1$	132.2	137.9	134.3	134.3	133.1
C_2-N_2	1.368	1.373	1.332	1.346	1.330	$C_2-N_2-O_2$	108.3	100.0	106.3	105.6	107.2
N_1-O_2	1.321	1.313	1.381	1.375	1.369	$N_1-O_1-N_2$	104.7	107.2	111.7	110.4	104.9
N_2-O_2	1.312	1.625	1.424	1.435	1.361	$N_1-C_1-C_6$	133.5	130.3	110.1	132.2	132.9
N_2-O_1	1.207	1.212	1.234	1.220	1.211	$C_1-N_1-O_2$	111.1	109.9	105.0	105.5	111.0
C_6-N_3	1.446	1.467	1.469	1.462	1.446	$C_6-N_3-O_3$	116.8	116.6	116.4	116.8	116.7
N_3-O_3	1.188	1.243	1.229	1.228	1.207	$C_6-N_3-O_4$	117.7	117.7	117.6	117.7	117.7
N_3-O_4	1.196	1.241	1.232	1.232	1.212	$C_2-C_3-H_1$	120.2	120.8	120.3	120.3	120.3
C_3-H_1	1.073	1.087	1.087	1.085	1.076	$C_3-C_4-H_2$	121.0	119.5	120.5	120.3	120.6
C_4-H_2	1.073	1.086	1.087	1.084	1.076	$C_6-C_5-H_3$	118.1	118.3	118.3	117.6	117.7
C_5-H_3	1.073	1.087	1.086	1.084	1.076						

[a] Bond lengths are in Å and angles in deg. [b] MP4(SDQ), no triple excitations. [c] BH&H denotes the BH&H−LYP exchange correlation functional.

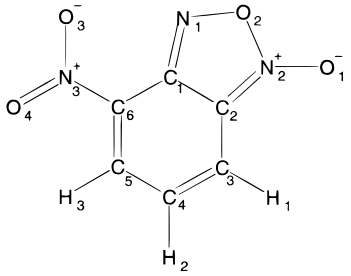

Figure 5. The atomic labeling of 4-nitrobenzofuroxan.

structures [N_1-O_2, 1.375 (B3-LYP) and 1.381 Å (MP4); and N_2-O_2, 1.435 (B3-LYP) and 1.424 Å (MP4)]. Note that the unsubstituted benzofuroxan optimized at the B3-LYP/6-311G-(d,p) level is in remarkably good agreement with crystallographic data.[21] MP2 significantly overestimates the N_2-O_2 bond of **1**, while RHF leads to an underestimation. To a lesser extent BH&H-LYP also underestimates this bond length. Resembling the RHF results, this functional leads to almost an identical length for the neighboring N_1-O_2 bond. Although these values appear to be too short for both bonds, the finding of almost identical bond lengths reflects the experimental results for 4,6-dinitrobenzofuroxan[58] (N_1-O_2, 1.42 Å; and N_2-O_2, 1.41 Å). It must be noted here that for other substituents than nitro groups the difference in the two bond lengths under consideration is more pronounced and may thus be specific for this particular substitution pattern. However, the BH&H-LYP functional fails to reproduce the experimentally known structure of unsubstituted benzofuroxan reliably.[61] For this molecule the functional also predicts almost identical bond lengths, while the two bonds differ by more than 0.08 Å experimentally. Therefore, structures including a furazan ring are not well represented by the hybrid BH&H-LYP functional. But, as will be shown below, the discussed differences in these geometric parameters have very little influence on relative energies and therefore BH&H-LYP energies may still be accurate in energetic considerations.

To test for basis set effects, the structure of **1** was also optimized by using Pople's 6-311+G* and 6-311G(2df,p) bases. Only very minor effects (≤0.007 Å) can been seen and thus the 6-31G* structure must be considered reliable. At the B3-LYP/6-311+G* level the N_1-O_2 and N_2-O_2 bond lengths are 1.370 and 1.436 Å and at the B3-LYP/6-311G(2df,p) level these parameters are 1.370 and 1.429 Å, respectively.

(61) Eckert, F.; Rauhut, G. Unpublished results.

Table 2. Relative Energies[a] of Structures Involved in Reaction Path A[b]

		TS1	
energy	geometry	E_{rel}	E_{rel}^{scal}
RHF	RHF	21.45	19.65
MP2	MP2	43.46	43.13
MP4(SDQ)	MP4(SDQ)	31.35	30.47
B3-LYP	B3-LYP	23.92	23.05
BH&H-LYP	BH&H-LYP	27.67	26.29
MP4(SDTQ)	MP4(SDQ)	31.87	30.99
CCSD	MP4(SDQ)	30.73	29.85
CCSD(T)	MP4(SDQ)	28.73	27.85
MP4(SDQ)	B3-LYP	30.94	30.06
MP4(SDTQ)	B3-LYP	32.09	31.21
CCSD	B3-LYP	30.62	29.74
BH&H-LYP	B3-LYP	27.01	26.13

[a] E_{rel}: energies relative to structure **1** (in kcal/mol), not corrected for zero-point vibrational energies. E_{rel}^{scal}: energies relative to structure **1** (in kcal/mol). Values have been corrected by scaled ZPEs; scaling factors taken to be 0.963 for B3-LYP, 0.943 for MP2, and 0.895 for RHF. For BH&H-LYP unscaled ZPE values have been used. MP4(SDQ), MP4(SDTQ), CCSD, and CCSD(T) energies have been corrected by scaled B3-LYP ZPEs. [b] Absolute energies and zero-point vibrational energies (ZPE) for all calculations presented in this table are provided in the Supporting Information.

The transition state involved in reaction mechanism A is of C_{2v} symmetry with a simultaneous cleavage of the N_1-O_2 bond and a new bond between the oxygen of the nitro group O_3 and the nitrogen N_1 of the furazan ring. The distances between these atoms at the B3-LYP/6-31G* and MP4(SDQ)/6-31G* levels are very similar, 1.996 and 2.002 Å. The RHF, MP2, and BH&H-LYP values differ slightly more (RHF, 2.160 Å; MP2, 1.908 Å; BH&H-LYP, 1.947 Å). The differences for the critical bond N_1-O_2 diminish for this structure and now MP2 is in the same range as B3-LYP and MP4(SDQ) (B3-LYP, 1.275 Å; BH&H-LYP, 1.234 Å; MP4(SDQ), 1.268 Å; MP2, 1.282 Å; RHF, 1.208 Å).

3.2. Energies. Relative energies for the structures involved in mechanism A are presented in Table 2 and are shown graphically in Figure 6. These energies were corrected for zero-point vibrational energies (ZPE). Calculations based on MP4-(SDQ) geometries were corrected by ZPEs computed at the B3-LYP, level, since this functional is especially well suited for the calculation of vibrational frequencies. ZPEs were scaled by factors as provided by Scott and Radom[31] and others.[29,62,63] Since

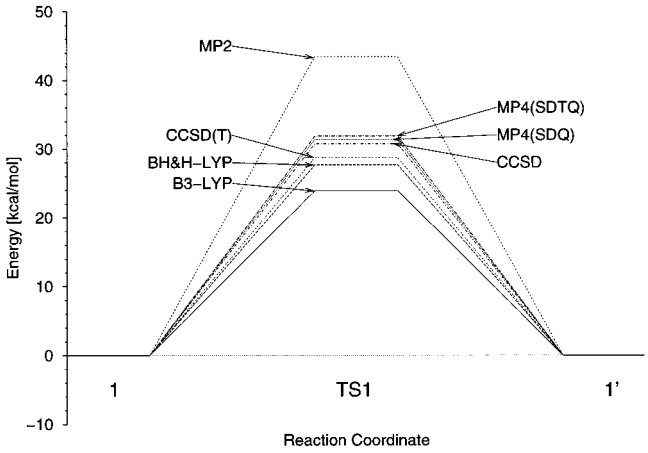

Figure 6. Energy profile for reaction path A at different theoretical levels. The profile is not corrected for ZPE effects. MP4(SDQ), MP4(SDTQ), CCSD, and CCSD(T) energies refer to geometries optimized at the MP4(SDQ) level.

scaling factors are not available for BH&H-LYP frequencies, the corresponding ZPEs were not adjusted.

The activation energies for this one-step mechanism vary between 19.7 and 43.1 kcal/mol for the different theoretical levels. Due to the insufficient description of the structural parameters and the rather low level of incorporating electron correlation effects, the RHF and MP2 activation energies must be considered erroneous. Furthermore, as stated by Truong *et al.*,[37−39] BH&H-LYP is believed to provide more accurate reaction barriers than the B3-LYP functional. This statement is in agreement with our findings that BH&H-LYP resembles more closely the CCSD(T) results than B3-LYP does. As discussed in the previous section, BH&H-LYP geometries are less reliable than B3-LYP or MP4(SDQ) geometries. However, as BH&H-LYP single-point calculations on top of B3-LYP geometries show, this has very little impact (0.2 kcal/mol) on the activation barrier. The same applies to MP4(SDTQ) and CCSD(T) single-point calculations on top of structures optimized at the MP4(SDQ) and B3-LYP levels, respectively. For these calculations, differences in activation energies are again as low as 0.2 kcal/mol (without considering ZPE effects). This justifies the use of B3-LYP geometries as reference structures for reaction mechanisms of type A instead of the computationally very demanding MP4(SDQ) geometry optimizations.

CCSD activation energies are essentially identical with MP4(SDQ) barriers, but the triples correction shifts them in opposite directions. On the basis of the MP4(SDQ) geometry, an increase of 0.5 kcal/mol is observed for the MP4(SDTQ) single-point calculations, while a lowering of 2.0 kcal/mol can be seen for CCSD(T) calculations. Basis set effects must be considered small, because MP4(SDQ)/6-311G(2df,p) calculations for 4-nitrobenzofuroxan (**1**) and transition state **TS1** shift the barrier up by less than 1 kcal/mol to 31.0 kcal/mol (in comparison to 30.1 kcal/mol at the MP4(SDQ)/6-31G* level). This again justifies the relatively small 6-31G* basis. Assuming the CCSD(T)/6-31G*//MP4(SDQ)/6-31G* activation barrier of 28.7 kcal/mol to be most accurate and the ZPE correction best represented by B3-LYP calculations, the barrier for reaction A is found to be 27.9 kcal/mol (ZPEs scaled by 0.963). This value is in surprisingly good agreement with the BH&H-LYP energy (26.3 kcal/mol). In summary, the barrier is ∼28 kcal/mol with a deviation less than ±10%, which may account for the basis set effects discussed above.

Due to the broad scattering of the activation energies and the unusually large differences in the N_2-O_2 bond lengths at the different theoretical levels, one is tempted to assume that multiconfigurational methods (CASPT2, MRCI) may provide more accurate results. To test for multiconfigurational effects, the T_1 diagnostic of Lee and Taylor[64,65] was applied to the CCSD calculations. They use the Euclidian norm of the single excitation cluster amplitudes in CCSD wavefunctions scaled by the number of electrons as a criterion to judge whether nondynamical correlation effects are large enough to cast doubt on single-reference calculations. They state that a T_1 value larger than 0.02 at the basis set limit probably indicates the need for a multiconfigurational electron correlation procedure. The T_1 values for CCSD calculations of **1** and **TS1** are 0.021 and 0.027, respectively. However, even though both values are above the recommended threshold, two arguments essentially refute the need for a multiconfigurational approach: First, since T_1 values decrease with growing size of the basis set (values up to 0.005 are reported[64]), these values computed with the small 6-31G* valence double-ζ basis will be smaller in the basis set limit and thus both structures must be considered to be at the edge of a one-determinantal treatment, but are probably still safe to be treated by the methods used above. Second, Taylor states that corrections for triple excitations substantially increase the radius of convergence of the coupled cluster method. Good agreement was found between CCSD(T) and MCSCF/MRCI calculations when T_1 was as large as 0.04. Since triple excitations have been taken into account in this study, we do not expect significant changes of our results at multiconfigurational levels of theory.

4. Reaction Path B

The alternative mechanism B as depicted in Figure 4 involves two symmetry-unique intermediates and two transition states. In principle, a larger number of local minima can be found on this potential energy surface because the nitroso groups and the nitro group allow rotations relative to the ring plane. By analogy, further saddle points can be found which belong to the rotation of these groups. Although interconversion of several conformers appears feasible for these floppy molecules, these rotational barriers are without relevance for the reaction mechanism under consideration. Therefore, we have limited our study to those structures in which the nitroso groups point in the same direction (i.e., above or below the ring plane). We found these conformers lowest in energy.

4.1. Geometries. The structures of intermediates **3** and **4** are shown in Tables 3 and 4. Since these structures do not include the heterocyclic furazan ring, one should expect better agreement within the set of different theoretical levels. This indeed is reflected in the geometrical parameters provided in Tables 3 and 4. Structural differences due to the computational methods are mainly dominated by general trends rather than by a limited number of exceptional bond lengths. The results show that bond lengths computed with the BH&H-LYP functional are consistently shorter (about 0.01 Å) than those calculated with the B3-LYP functional, the latter usually being in excellent agreement with experimental results.[66] As can be expected, the largest differences are in the soft rotational degrees of freedom of the nitroso and nitro groups (CCNO) and thus small correlation effects may cause large amplitude motions. Consequently, the RHF geometry must be considered erroneous. Therefore, the

(62) Hout, R.; Levi, B.; Hehre, W. *J. Comput. Chem.* **1982**, 3, 234.
(63) DeFrees, D.; McLean, A. *J. Chem. Phys.* **1985**, *82*, 333.
(64) Lee, T.; Taylor, P. *Int. J. Quantum Chem. Symp.* **1989**, *23*, 199.
(65) Taylor, P. Accurate Calculations and Calibration. In *Lecture Notes in Chemistry*, Roos, B., Ed.; Springer Verlag: Heidelberg, 1992; Vol. 58.
(66) Johnson, B.; Gill, P.; Pople, J. *J. Chem. Phys.* **1993**, *98*, 5612.

Table 3. Geometric Parameters of 1,2-Dinitroso-3-nitrobenzene (**2**: C_1, MP2, MP4(SDQ), B3-LYP, BH&H-LYP; and C_s, RHF)

r^a	RHF	MP2	MP4[b]	B3-LYP	BH&HC	angles[a]	RHF	MP2	MP4b	B3-LYP	BH&H[c]
C_1-C_2	1.403	1.405	1.398	1.409	1.393	$C_1-C_2-C_3$	120.9	120.8	120.9	120.3	120.6
C_2-C_3	1.388	1.398	1.398	1.401	1.390	$C_2-C_3-C_4$	120.7	119.7	119.9	120.0	120.2
C_3-C_4	1.376	1.394	1.392	1.390	1.380	$C_3-C_4-C_5$	119.6	120.5	120.2	120.4	119.9
C_4-C_5	1.380	1.398	1.398	1.401	1.387	$C_4-C_5-C_6$	120.3	118.8	118.9	119.3	119.4
C_5-C_6	1.385	1.390	1.389	1.387	1.380	$C_5-C_6-C_1$	121.3	122.2	122.1	121.5	121.8
C_6-C_1	1.405	1.398	1.397	1.403	1.390	$C_6-C_1-C_2$	117.2	117.9	117.9	118.5	118.0
C_1-N_1	1.465	1.451	1.476	1.434	1.446	$C_2-N_2-O_1$	113.6	112.5	112.7	115.1	113.8
C_2-N_2	1.459	1.456	1.472	1.443	1.441	$C_2-N_2-O_2$	81.2	81.0	80.0	82.7	80.0
N_1-O_2	1.172	1.243	1.222	1.217	1.191	$N_1-C_1-C_2$	125.3	121.4	121.3	119.1	120.9
N_2-O_1	1.177	1.240	1.225	1.217	1.196	$N_1-O_2-N_2$	97.2	88.7	84.6	93.6	85.2
C_6-N_3	1.481	1.464	1.472	1.473	1.456	$C_1-N_1-O_2$	115.7	112.0	112.5	113.4	113.7
N_3-O_3	1.184	1.243	1.232	1.228	1.208	$C_6-N_3-O_3$	119.9	116.9	116.9	117.1	117.2
N_3-O_4	1.197	1.242	1.232	1.229	1.209	$C_6-N_3-O_4$	115.8	117.0	117.1	117.0	117.2
C_3-H_1	1.071	1.087	1.087	1.086	1.076	$C_2-C_3-H_1$	118.5	118.6	118.6	118.1	118.1
C_4-H_2	1.074	1.087	1.087	1.086	1.077	$C_3-C_4-H_2$	120.5	120.0	120.1	120.1	120.3
C_5-H_3	1.069	1.086	1.086	1.083	1.075	$C_6-C_5-H_3$	119.0	119.3	119.3	119.3	118.9
						$O_2-N_1-C_1-C_2$	0.0	−39.8	−48.3	−30.5	−46.4
						$O_1-N_2-C_2-C_3$	0.0	−32.8	−24.3	−37.5	−23.8
						$O_3-N_3-C_6-C_1$	0.0	−31.9	−27.6	−24.2	−23.4
						$O_4-N_3-C_6-C_1$	180.0	149.1	153.3	156.5	157.6

[a] Bond lengths are in Å and angles in deg. [b] MP4(SDQ), no triple excitations. [c] BH&H denotes the BH&H-LYP exchange correlation functional.

Table 4. Geometric Parameters of 1,3-Dinitroso-2-nitrobenzene (**3**: C_{2v}, RHF, MP4(SDQ), B3-LYP, BH&H-LYP; and C_2, MP2)

r^a	RHF	MP2	MP4[b]	B3-LYP	BH&H[c]	angle[a]	RHF	MP2	MP4[b]	B3-LYP	BH&H[c]
C_1-C_2	1.381	1.395	1.391	1.395	1.383	$C_1-C_2-C_3$	119.4	119.7	119.7	119.5	119.5
C_2-C_3	1.388	1.398	1.396	1.400	1.388	$C_2-C_3-C_4$	120.1	119.8	119.8	120.3	120.1
C_3-C_4	1.384	1.396	1.396	1.394	1.384	$C_3-C_4-C_5$	120.1	120.5	120.3	119.9	120.0
C_1-N_1	1.465	1.464	1.474	1.481	1.465	$C_6-C_1-C_2$	120.0	120.5	120.7	120.6	120.7
C_2-N_2	1.438	1.454	1.465	1.451	1.436	$C_1-N_1-O_2$	116.4	116.3	116.2	116.2	116.3
N_1-O_2	1.187	1.241	1.228	1.223	1.203	$C_2-N_2-O_1$	114.7	113.0	113.4	114.1	114.3
N_2-O_1	1.177	1.240	1.224	1.216	1.195	$N_1-C_1-C_2$	119.5	119.7	119.6	119.7	119.6
C_3-H_1	1.073	1.087	1.087	1.086	1.076	$C_2-C_3-H_1$	118.7	118.4	118.6	117.7	118.1
C_4-H_2	1.074	1.087	1.087	1.086	1.077	$C_3-C_4-H_2$	119.9	119.8	119.8	120.1	120.0
						$C_2-C_1-N_1-O_2$	90.0	72.5	90.0	90.0	90.0
						$C_1-C_2-N_2-O_1$	180.0	180.4	180.0	180.0	180.0

[a] Bond lengths are in Å and angles in deg. [b] MP4(SDQ), no triple excitations. [c] BH&H denotes the BH&H-LYP exchange correlation functional.

C_s symmetry of the RHF structure of intermediate **3** certainly is wrong and most likely must be expected to be a rotational saddle point at correlation including levels. At the B3-LYP, BH&H-LYP, and RHF levels intermediate **4** shows C_{2v} symmetry, while the MP2 calculation results in C_2. Due to sterical hindrance of the nitroso groups, the nitro group stands perpendicular to the ring plane. Figure 7 shows the structure of the B3-LYP optimized intermediate **4**. Note that both intermediates have several soft modes and therefore have very flat potential energy surfaces, which makes it quite difficult to assign a definite structure to these molecules. This also explains the difficulties in assigning a single molecular point group to these structures, since small numerical inaccuracies or low iteration thresholds can easily cause the loss of a symmetry element. All transition states and intermediates have been verified by frequency calculations and following the IRC reaction path.

4.2. Energies. Energies for reaction B are given in Table 5 and are visualized in Figure 8. As can be expected for this mechanism, this reaction path is dominated by transition state **TS3**, i.e., the electrophilic attack of the nitroso group toward the oxygen of the nitro group. Since the same arguments hold as for reaction A, the CCSD(T) activation energies must be considered as the most accurate. However, an unusually broad scattering of the activation barrier was found for transition state **TS2** (cf. Table 5). Relative energies based on B3-LYP geometries are significantly below the corresponding values referring to MP4(SDQ) structures, which we consider to be more reliable. This indicates that B3-LYP fails to describe **TS2** correctly.

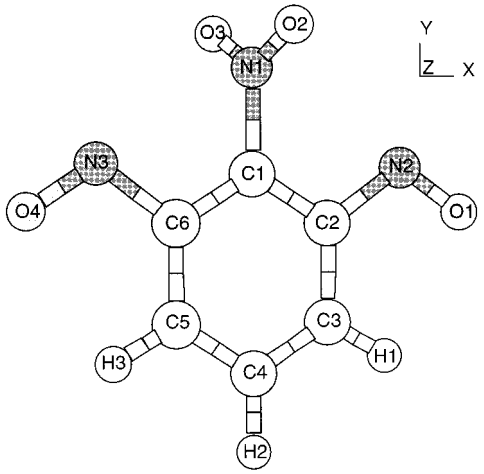

Figure 7. Structure of intermediate **4** optimized at the B3-LYP/6-31G* level (C_{2v} symmetry). View of the molecule rotated 30° around the *y* axis.

Although IRC calculations confirmed that the transition state found at the B3-LYP level is correct, the potential energy hypersurface was carefully checked for other, similar transition states. However, no further stationary points could be found. Since this transition state is not the rate-determing step of reaction B, this result has little impact on the discussion of the mechanisms investigated here. However, the bond-breaking process characterized by **TS2** is the same as in the ring-chain

Table 5. Relative Energies[a] of Structures Involved in Reaction Path B[b]

		3		**4**		**TS2**		**TS3**	
energy	geometry	E_{rel}	E_{rel}^{scal}	E_{rel}	E_{rel}^{scal}	E_{rel}	E_{rel}^{scal}	E_{rel}	E_{rel}^{scal}
RHF	RHF	−10.26	−12.56	−11.11	−13.56	30.77	28.92	53.95	51.17
MP2	MP2	17.29	15.84	16.88	15.03	25.77	24.74	49.00	47.65
MP4(SDQ)	MP4(SDQ)	2.53	0.63	2.00	−0.11	20.54	18.75	45.46	43.12
B3-LYP	B3-LYP	16.22	14.32	16.46	14.35	16.59	14.80	40.26	37.92
BH&H-LYP	BH&H-LYP	8.69	6.48	8.29	5.90	22.24	20.40	47.53	44.77
CCSD	B3-LYP	3.31	1.41	1.43	−0.68	10.81	9.02	45.39	43.05
CCSD	MP4(SDQ)	1.94	0.04	1.71	−0.40	18.09	16.30	45.31	42.97
CCSD(T)	MP4(SDQ)	6.43	4.46	6.38	4.19	13.44	11.58	41.19	38.76

[a]Notation and parameters as in Table 2. [b] Absolute energies and zero-point vibrational energies (ZPE) for all calculations presented in this table are provided in the Supporting Information.

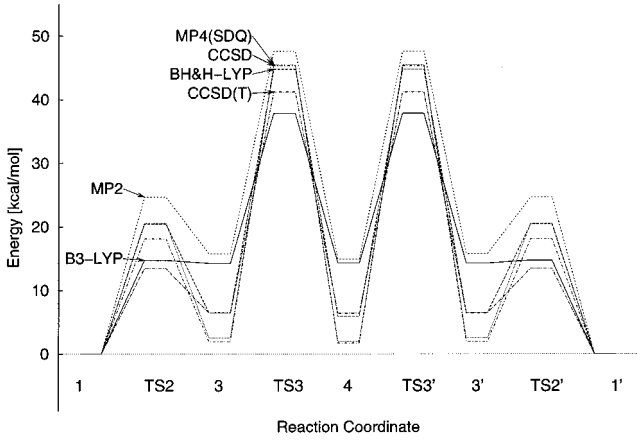

Figure 8. Energy profile for reaction path B at different theoretical levels. The profile is not corrected for ZPE effects. MP4(SDQ) and CCSD energies refer to geometries optimized at the MP4(SDQ) level.

tautomerism of unsubstituted benzofuroxan investigated recently.[21] Since these studies relied on B3-LYP calculations which significantly underestimate this barrier, it is most likely that this bond cleavage will be the rate-determing step for this related reaction. Therefore, the reaction mechanism of the ring-chain tautomerism needs to be reinvestigated at least at the MP4-(SDQ) level.

The rate-determing step of reaction B is characterized by transition state **TS3**. All calculations which may be used for reliable energy discussions (see above) yield a barrier above 38 kcal/mol (cf. Table 5). This value is 10 kcal/mol higher than the most accurate estimation of the activation energy computed for reaction A. Even allowing for a considerable uncertainty in the computed barriers, the conclusion must be that mechanism A is the preferred reaction path. Considering the relative energies of 1,2-dinitroso-3-nitrobenzene (**3)** and 1,2-dinitroso-3-nitrobenzene (**4**), the tautomer with higher symmetry **4** is most likely more stable than the asymmetric one **3**.

5. Conclusions

A prototype reaction of the Boulton−Katritzky rearrangement (BKR) has been investigated by means of *ab initio* and density functional theory. All stationary points of two possible reaction mechanisms (Figures 3 and 4) have been computed at different theoretical levels. Although the scattering of relative energies (activation barriers, stabilization energies) is unusually broad, this study definitely indicates an unimolecular one-step mechanism for the BKR. The rather high activation energy, estimated from CCSD(T)/6-31G*//MP4(SDQ)/6-31G* calculations to be 28 kcal/mol ±10%, is in agreement with experimental NMR results. Harris *et al.*[67] found that the ABC pattern of the proton NMR spectrum of 4-nitrobenzofuroxan does not alter toward a time averaged AB_2 pattern even at temperatures up to 160 °C, indicating that fast tautomerism does not occur. Using Eyring's equation they estimate a free energy of activation higher than 20 kcal/mol. On the contrary, the conversion of 5-methyl-4-nitrobenzofuroxan to 7-methyl-4-nitrobenzofuroxan takes place on gentle heating, revealing that effects due to substituents result in an exothermic reaction. A computational study on the influence of different substituents on the BKR is in progress.[68] A tricyclic intermediate, already rejected by Katritzky and Gordeev,[6] could not be trapped by the methods used here. Since dipole moments (see Table 6) for transition states involved in mechanism B are slightly lower than the one for **TS1**, we do not expect a change of the mechanism due to solvent effects.

Table 6. DFT Derived Dipole Moments [D] for Structures Involved in Reaction Mechanisms A and B

structure	B3-LYP	BH&H-LYP
1	5.58	5.81
TS1	5.76	5.98
3	5.37	5.55
4	5.96	6.25
TS2	5.43	5.78
TS3	5.61	5.86

Moreover, this study confirms the general findings of Truong *et al.* that BH&H-LYP reaction barriers are in better agreement with CCSD energies than B3-LYP, which fails to describe the transition state of the furazan ring opening. Unfortunately, the BH&H-LYP functional predicts too short bond lengths and is thus less reliable for the investigation of structural parameters.

Acknowledgment. Computer time on the SGI PowerChallenge of the Institut für Theoretische Chemie (Stuttgart) is kindly acknowledged. Moreover, we thank the High-Performance Computing Center for Science and Industry Stuttgart for computation time on the NEC-SX4.

Supporting Information Available: Tables of absolute energies and zero-point vibrational energies of structures involved in reaction paths A and B (2 pages, print/PDF). See any current masthead page of ordering and Internet access instructions.

JA981720X

(67) Harris, R. K.; Katritzky, A. R.; Øksne, S.; Bailey, A. S.; Paterson, W. G. *J. Chem. Soc.* **1963**, 197.

(68) Eckert, F.; Rauhut, G.; Steel, P. J.; Katritzky, A. R. Manuscript in preparation.